

Interaction Between a Conical Shock Wave and a Plane Turbulent Boundary Layer

S. L. Gai*

Australian Defence Force Academy, Canberra, Australian Capital Territory 2600, Australia
and

S. L. Teh†

Nanyang Technological University, Singapore 639798, Republic of Singapore

An investigation into the interaction between an incident conical shock wave and a plane two-dimensional turbulent boundary layer is reported. The study has provided information on the interaction pattern and the surface flowfield under both attached and separated flow conditions. The existence of significant pressure gradients in the spanwise direction after the shock leads to strong crossflows. A horseshoe pattern of separation whose strength and size are reduced away from the plane of symmetry is identified. The interaction produces upstream influence, which is curved as a result of decreasing influence of the conical shock away from the plane of symmetry. Incipient separation is inferred, and it is shown that criteria for its existence are similar to other three-dimensional interactions.

I. Introduction

A FAIR degree of understanding of three-dimensional shock wave/boundary-layer interaction has been achieved in recent years, but the majority of these studies have generally been confined to what are known as glancing or swept-shock interactions (see for example, Refs. 1 and 2). An interesting three-dimensional interaction problem is that of an interaction between an incident conical shock and a two-dimensional turbulent boundary layer on a plane surface. This problem has practical relevance, for example, in side intakes with center bodies of supersonic aircraft and ramjets. A literature review has shown that very few studies, for example, Migotsky and Morkovin's³ inviscid analysis of three-dimensional shock-wave reflections and Panov's⁴ experimental study of conical shock/two-dimensional boundary-layer interaction, exist in the open literature. However, related problems, those of an incident conical shock interacting with an axisymmetric turbulent boundary layer developed on a cylindrical surface⁵ and the interaction of a plane shock wave with a turbulent boundary layer on an axial cylinder,⁶ have been studied.

This paper presents the results of an interaction between a conical shock wave and a two-dimensional turbulent boundary layer on a flat plate at a freestream Mach number of 2.0. The interaction strength and scale were varied by varying the cone angle as well as the height of the cone above the plate. Particular attention is given to crossflows caused by the interaction up to separation and beyond. The problem belongs to one of a class of dimensionless interactions as defined by Settles and Dolling.²

II. Experimental Arrangement and Data Acquisition

The experiments were conducted in a blow-down supersonic wind tunnel of cross section 155×90 mm at a freestream Mach number 2.0 and two freestream unit Reynolds numbers 30×10^6 and 58×10^6 per meter. All of the results discussed in this paper were obtained at a unit Reynolds number of 30×10^6 per meter. Similar results obtained at a unit Reynolds number of 58×10^6 per meter showed no significant differences with regard to both separation and upstream influence.

The models consisted of cones with half-angles θ_c ranging from 14 to 30 deg. The cone base diameter was 20 mm. The flat plate was 279 mm long, 90 mm wide, and 9 mm thick with a sharp leading edge. Figure 1 shows the schematic of the experimental arrangement. In all of the cases, the plate was aligned with the freestream, and the cones were at 0-deg angle of attack.

The techniques employed for acquisition of data consisted of schlieren photography, surface oil-flow visualization, and surface-pressure measurements.

The boundary layer δ_0 on the plate in the interaction region was measured and found to be turbulent with a thickness of the order of 2.4 mm. Its velocity profile closely followed the well-known one-seventh power law profile.

Preliminary investigations⁷ using flow visualization were conducted with 20-, 30-, and 40-deg half-angle cones mounted at heights h of 30, 45, and 60 mm. The cones were positioned in such a way that the shocks interacted with the flat plate boundary layer at the same location l_0 , 169 mm from the leading edge of the plate, thus providing a constant boundary-layer thickness at the beginning of the interaction with all of the cones.

These studies showed that the scale of the interaction depends not only on the freestream Mach number and the cone half-angle (that is, shock strength), but also on the cone length and the height at which the cone is mounted above the plate.^{4,6,8,9} In particular, depending on the cone angle and the height at which the cone is mounted above the flat plate, expansion waves originating from the base of the cone were observed to interact with either both the incident and the reflected shocks or with only the reflected shock.

Secondly, for a given cone angle, base diameter, and Mach number, whether separation occurred on the plate depended on the height of the cone above the plate. Figure 2 shows the results based on surface oil-flow studies.⁷ The uncertainty in the measurements based on oil-flow pictures is ± 10 –15%. In the figure the separation length at the plane of symmetry is shown normalized by the height of the cone above the plate and plotted against the cone half-angle θ_c . The scale of interaction for a given cone angle (and hence shock strength) is clearly governed by the height of the cone above the plate.

The detailed studies of the interaction reported next describe experiments with cones of half-angles ranging from 14 to 30 deg, but all mounted at a single height of 30 mm above the flat plate, which also ensured that the effect of expansion waves from the base of the cone did not interfere with the incident conical shock prior to the interaction with the boundary layer on the plate.⁹ There was a slight effect of expansion waves on the reflected shock, but it was well away from the plate surface.

Received 18 February 1998; revision received 24 August 1999; accepted for publication 18 September 1999. Copyright © 1999 by the American Institute of Aeronautics and Astronautics, Inc. All rights reserved.

*Associate Professor, University College, School of Aerospace and Mechanical Engineering, Associate Fellow AIAA.

†Senior Lecturer, Mechanical and Production Engineering.

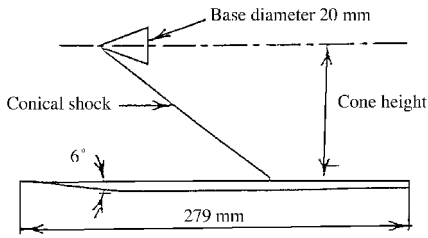


Fig. 1 Experimental arrangement.

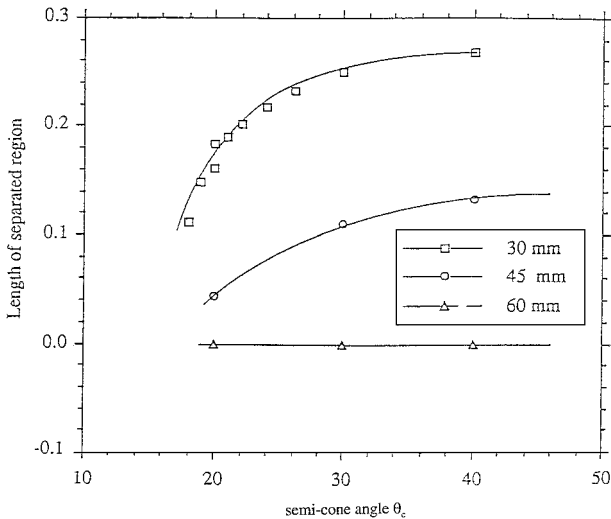


Fig. 2 Effect of height of the cone on separation length.

III. Results and Discussion

A. Flow Visualization

1. Schlieren Photographs

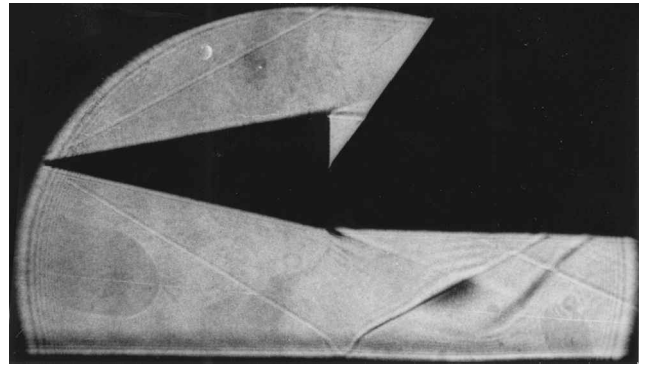
Figures 3a–3c show schlieren photographs of a conical shock interacting with a turbulent boundary layer on a flat plate. The knife edge was horizontal, and the photographic plane was positioned such that the image was focused on the central plane of the test section as determined using the thin lens equation.¹⁰ With this arrangement, while the density gradients normal to the plate are seen, the effects on density gradients along the spanwise and streamwise directions will not be apparent on the photographs.

Figure 3a shows a shock generated with a 14-deg half-angle cone. We can see clearly the incident shock, the boundary layer, and the reflected shock. The bright strip next to the plate is caused by reflections from the plate surface, and the boundary layer can be identified up to the outer edge of the grey horizontal strip. The incident shock becomes curved as it penetrates the boundary layer and is reflected again as a shock with pronounced curvature in the boundary layer. Such a weak interaction system is discussed by Henderson.¹¹ The expansion from the cone base has some influence on the reflected shock, but the interaction at the plate surface is unaffected.

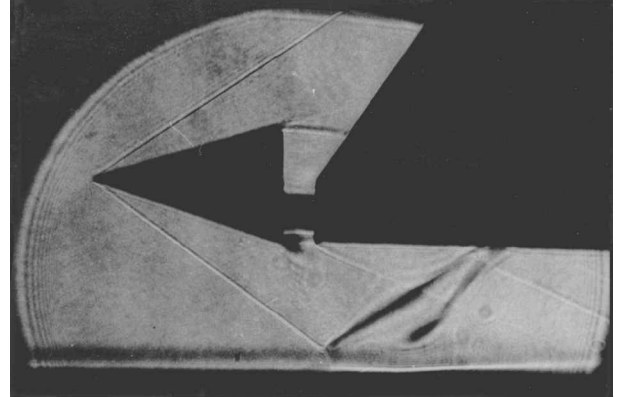
Figure 3b shows the case of an interaction with the shock generated by a 20-deg half-angle cone. With the stronger shock the boundary layer has thickened, and we can discern the formation of the reflected shock from the coalescence of compression waves formed within the boundary layer and ahead of the incident shock.¹² The reflected shock is followed immediately by expansion waves (dark patches), and this would indicate the presence of a small separation bubble. The existence of a separation bubble was further confirmed from surface oil-flow experiments, which will be discussed presently.

Figure 3c illustrates the case of a strong interaction with a 30-deg half-angle cone. We can see that the reflected shock is stronger and has extended upstream indicating a large separation bubble. We can also see the strong expansion as the flow is directed parallel to the plate by the reflected shock.^{11, 12}

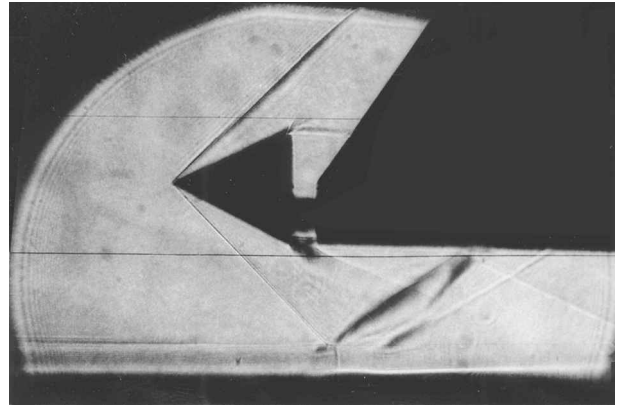
These interaction characteristics are very similar to those observed by Panov,⁴ who seems to be the only one to have conducted interaction studies using a configuration such as the present one.



a) $\theta_c = 14$ deg



b) $\theta_c = 20$ deg



c) $\theta_c = 30$ deg

Fig. 3 Schlieren photographs showing interaction at the symmetry plane with the cone height $h = 30$ mm above the plate.

2. Surface Oil-Flow Pictures

Figures 4a–4c show surface oil-flow patterns on the plate for interactions with cones of half-angles 16, 21, and 26 deg, respectively. These illustrate the evolution of the flowfield on the plate with increasing shock strength. They begin with an unseparated flow and go through to fully separated flow. Although the cone angles with which these oil-flow pictures were taken are slightly different from those of schlieren photographs, the flow situations they depict are very similar.

Considering Fig. 4a first; the incident shock footprint is shown to indicate its position. There is no deflection of streamlines at the line of symmetry. Away from the line of symmetry behind the shock, the surface streamlines go through large deflections initially and then become parallel because of side-wall constraint. The side-wall influence can be clearly seen.

Figure 4b shows the situation where the boundary layer on the plate has separated. We can identify separation as lines of coalescence¹³ separated by a bright patch. The attachment line is seen with a nodal point on the line of symmetry from where the

surface streamlines are seen to emanate (see, for example, Ref. 6). The separation and attachment lines curve downstream and are terminated by the side-wall constraint.

Figure 4c illustrates the case of a large separated region. Only one half of the plate surface is shown on this figure as the flow is symmetric. Once again, we note separation, attachment, and a curved separation region. However, in addition to the primary separation, there appears to be a secondary separation embedded within

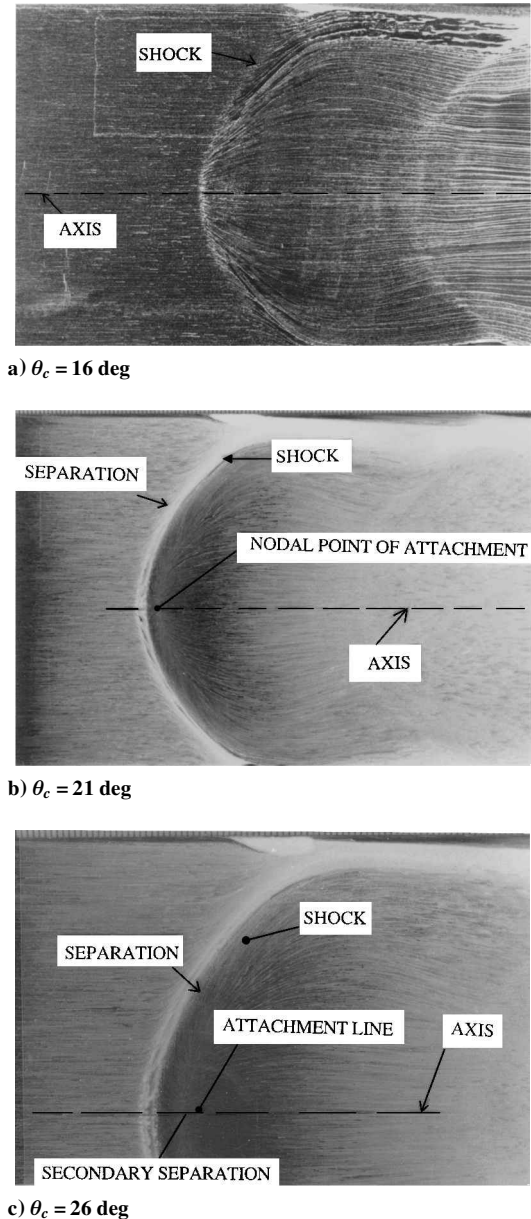


Fig. 4 Surface oil-flow patterns on the plate.

the primary separation zone. Such a feature has also been noted by Brosh et al.⁶ The strong side-wall influence is again seen.

The notable feature in Figs. 4b and 4c is the curved separation whose axis is normal to the flow direction in the plane of symmetry but bends along the spanwise direction, its axis ultimately becoming parallel to the flow direction. The curved separation gives rise to the well-known horseshoe vortex, which curls around on either side of the axis of symmetry. This vortex breaks down eventually: first, because of the lateral pressure gradient and second, because of the side-wall constraint. Accumulation of oil (seen as a bright patch) is indicative of this state of affairs. This type of separated flow picture is also observed in interactions with blunt fins and protuberances.^{1,2}

This surface flow pattern of the interaction is generally similar to that of Panov.⁴ Although Panov does not give the tunnel dimensions in his study, from the information given in his paper it is possible to deduce the interaction region of his study. If we consider the interaction aspect ratio defined as width of the plate/height of the cone above the plate, then this ratio is between four and five in his study, whereas it is three in the present case. Second, the boundary-layer development length up to the beginning of interaction l_0/δ_0 is approximately the same (74 in Panov's case and 70 in the present case). Thus, it is possible that side-wall effects might have been somewhat stronger here.

On the other hand, Panov does not elaborate on the importance of the influence of the expansion fan from the cone base. As we have shown, this influence can be significant on both the incident and reflected shocks. In fact, the only schlieren photograph in his paper shows that the incident shock is quite severely affected by the cone base expansion and so would undoubtedly have influenced the interaction region and the pressure distributions on the plate.

Panov also noted that separation was confined to the symmetry plane when the shock was not strong. This is consistent with the present study.

B. Pressure Measurements

Figure 5 shows the flat plate on which the surface pressure data were taken. The shaded region shows the interaction grid made up of seven data stations, spaced 6 mm apart, including the line of symmetry. The last station was 9 mm from the side wall. The pitch of the pressure orifices in the interaction region was 2 and 4 mm as shown. Whereas the bulk of these data were taken on one side of the symmetry axis, there were also pressure orifices located at a spanwise distance of 24 mm from the line of symmetry on the opposite side. These pressure taps served to check the symmetry of the flow. The pressures were measured by a pressure transducer connected to a Scanivalve. The accuracy of the pressure data is of the order of $\pm 0.5\%$.

Although the whole interaction region was provided with a total of 258 pressure orifices, the minimum pitch (2 mm) is still of the order of the boundary-layer thickness (2.4 mm), a somewhat coarse resolution. However, it is believed that all significant flow features are captured as pressure data are complemented by two different flow visualization data.

Figures 6a–6c show the pressure distributions in the interaction region for the 14, 20, and 30-deg half-angle cones at a freestream unit Reynolds number of 30×10^6 per meter. The footprint of the incident shock is also indicated.

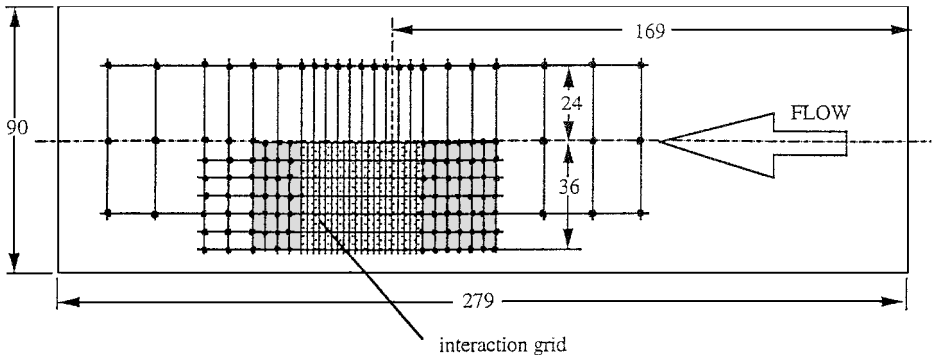
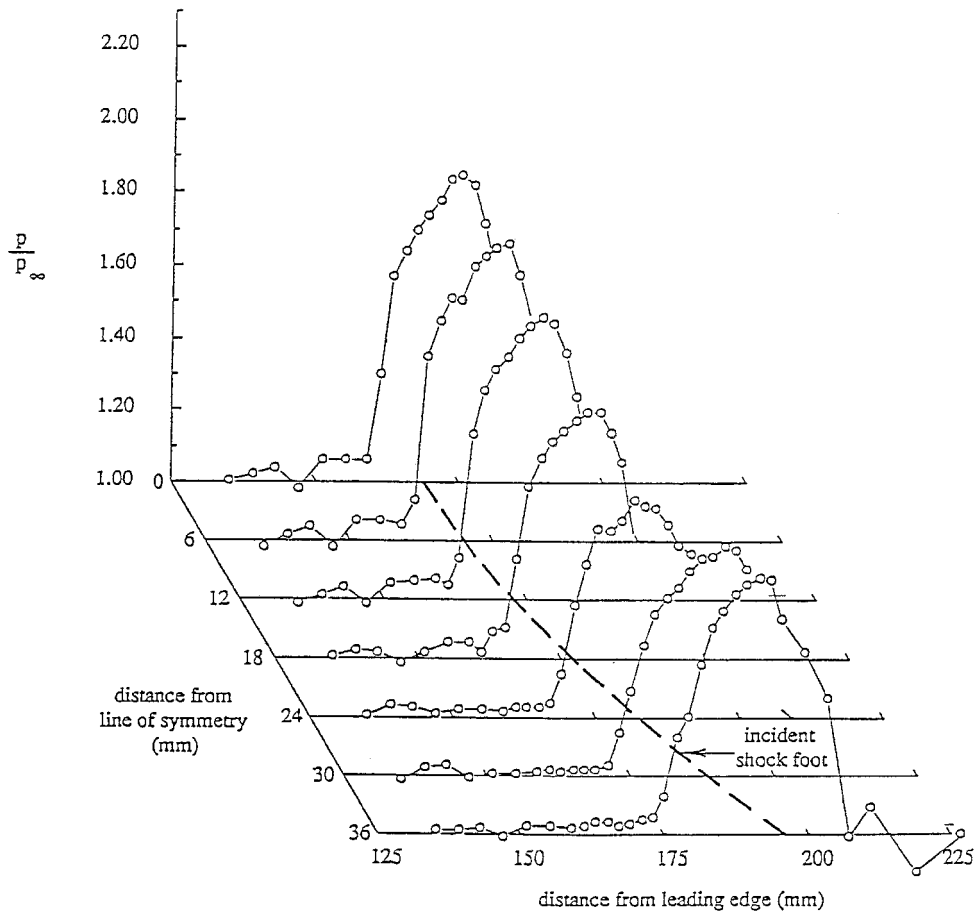
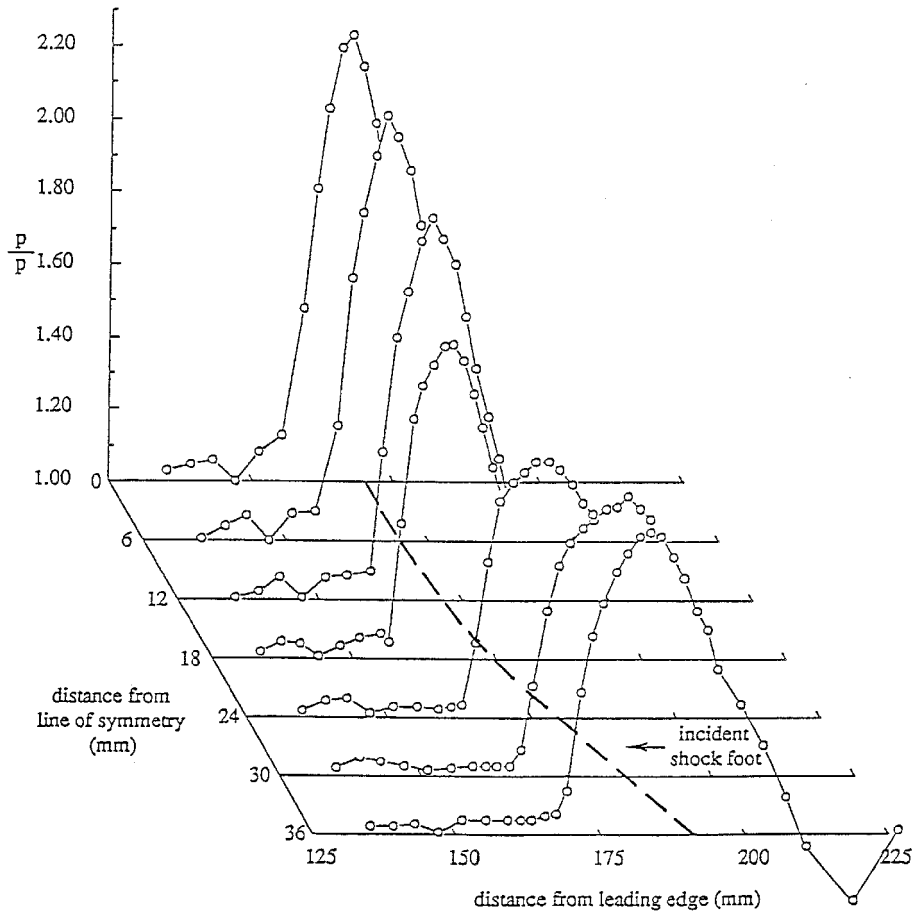


Fig. 5 Surface-pressure measurement grid (dimensions in millimeters).

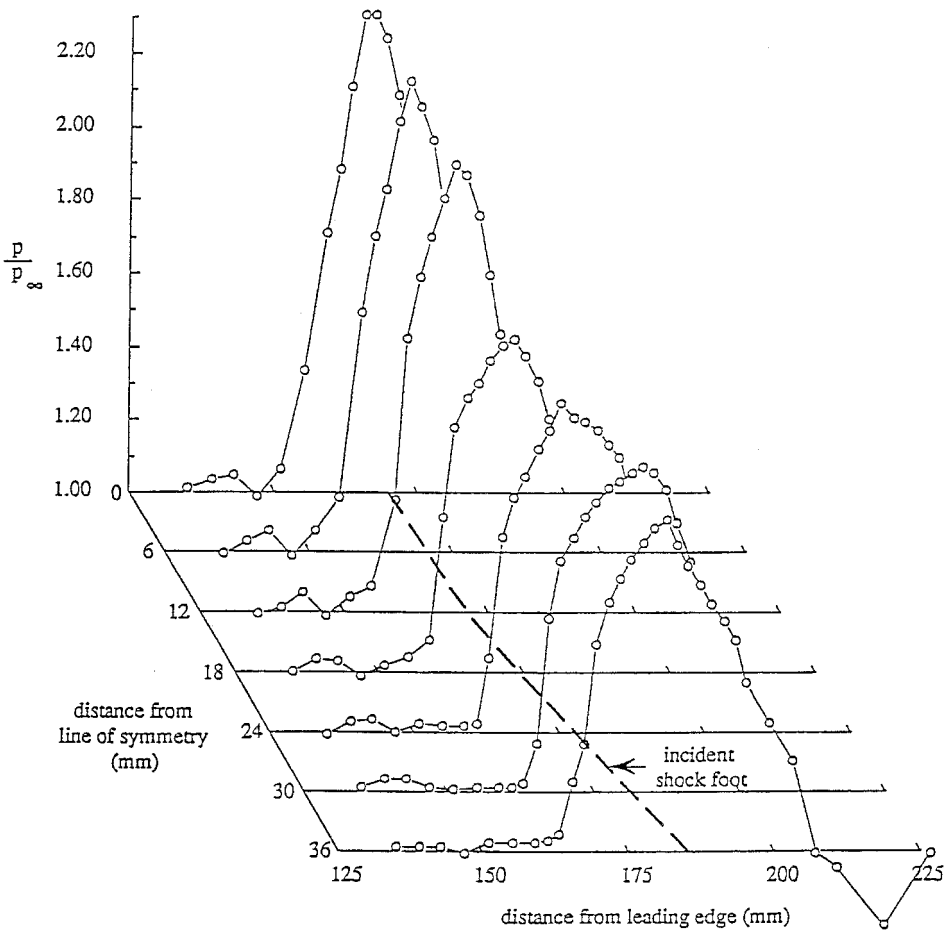


a) $\theta_c = 14^\circ$



b) $\theta_c = 20^\circ$

Fig. 6 Surface-pressure distributions in the interaction region.



c) $\theta_c = 30$ deg

Fig. 6 Surface-pressure distributions in the interaction region (continued).

In general, the surface pressures at all stations rise from the freestream pressure to a maximum after going through the incident and reflected shock system at the plate surface. However, they begin to rise at different streamwise distances from the leading edge of the plate. For example, with the 14-deg half-angle cone, Fig. 6a, the initial steep rise in pressure on the symmetry plane begins at 159 mm from the leading edge, whereas the pressure rise starts at 175 mm from the leading edge at 30 mm across in the spanwise direction. The corresponding values for the 20- and 30-deg half-angle cones are 151 and 165 mm and 147 and 163 mm, respectively.

The peak pressure rise decreases in the spanwise direction implying that the intensity of interaction decreases in the spanwise direction. Again, with the 14-deg half-angle cone, Fig. 6a, the peak pressure ratio on the symmetry plane is 1.85, whereas it reduces to 1.62 at 30 mm from the line of symmetry. The corresponding values for the 20- and 30-deg half-angle cones are 2.2 and 1.78 and 2.3 and 1.89, respectively.

These surface-pressure distributions are generally similar to those of Kussoy et al.⁵ As they noted, there is no indication of a pressure plateau associated with separation in the case of 20- and 30-deg half-angle cones, although the oil-flow studies showed that separation had just occurred with the 20-deg half-angle cone and that the flow was well separated with the 30-deg half-angle cone. Also, for the 30-deg half-angle cone, the pressure data do not show any clear indication of a secondary separation observed in the oil-flow studies.

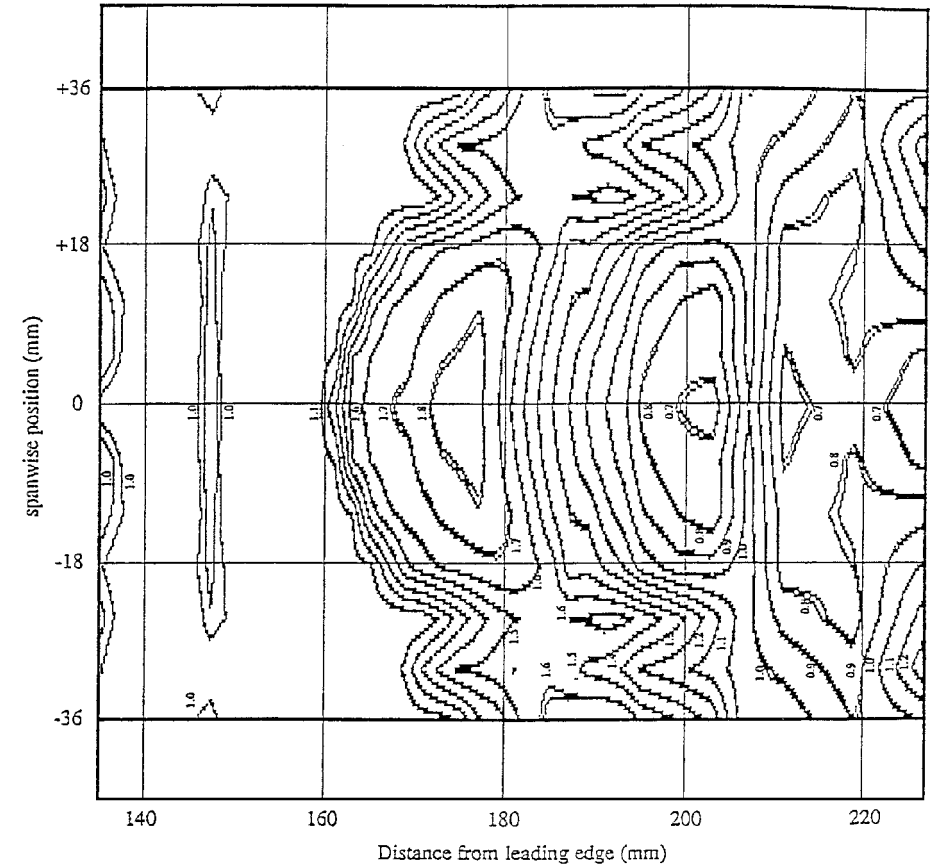
Concerning the surface-pressure distribution along the symmetry plane in the case of 20- and 30-deg half-angle cones, they do not exhibit the characteristic shape noted by Panov.⁴ Panov's data show a clear dip in the pressure distribution curve after the pressure rise at separation and prior to maximum pressure at reattachment. In fact, Panov infers that such a dip is indicative of a separation bubble. As pointed out by Settles and Dolling,² this type of interaction is quite akin to flowfield induced by blunt fin and circular cylinder on a plate. It is therefore quite possible that the dip in the pressure

distribution observed by Panov is indicative of secondary separation embedded in the primary separation. As indicated earlier, the likely reason for the absence of such a dip here is the rather coarse pitch of the pressure orifices in the interaction region.

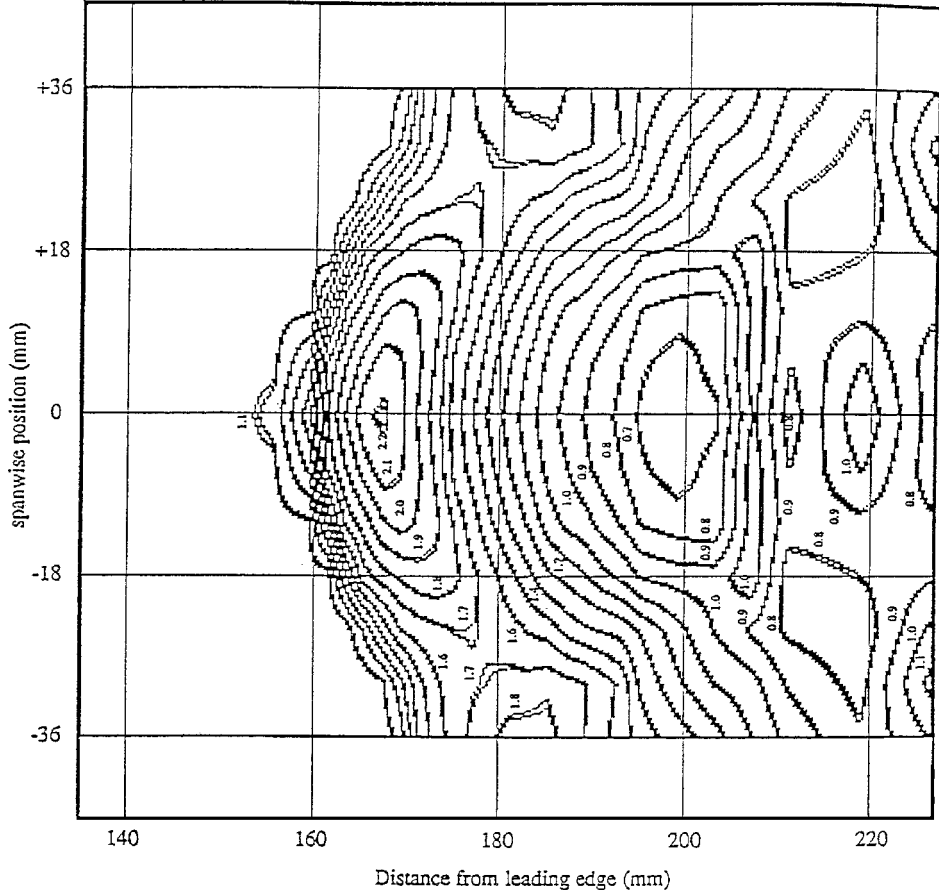
A feature that is unresolved in these figures is the unsteadiness in pressure readings upstream of the pressure rise. These fluctuations, maximum up to 7%, are present in all of the cases. The freestream static-pressure fluctuation was found to be of the order of 1 kHz while the frequency response of the measuring system was better than 67 kHz. The fact that these measurements were repeatable and also more predominant in the midspan region but not in the outer regions prompts one to speculate if this is a flow separation effect. However, this can be discounted because these disturbances occur well ahead of the beginning of interaction and are present even with the 14-deg half-angle cone.

Figures 7a–7c show isobars on the plate for the same cones. Although the heavier lines delineating the smaller rectangle in these figures represent the total interaction region studied, detailed measurements were taken only in the lower half of the rectangle as mentioned earlier. The contours shown in the upper half are drawn assuming symmetry of the flow. Typically, densely grouped pressure contours with increasing magnitude in the shock front region indicate compression of the flow. On reaching a maximum value after the attachment line, the pressures decrease as a result of expansion. The severe pressure gradients in the footprint region of the shock show the spread of interaction in the lateral direction indicating strong crossflows. These features are consistent with oil-flow pictures both in regard to spread of interaction and flow symmetry.

These isobars also give an indication of the side-wall effects. This is seen by the irregular curvature in the outer regions of pressure contours of the 14-deg half-angle cone and the straightening out of these contours caused by the lateral spreading of the interaction in the case of the larger cone angles. The estimation is made that the side-wall effects extend approximately 15 mm inward from the

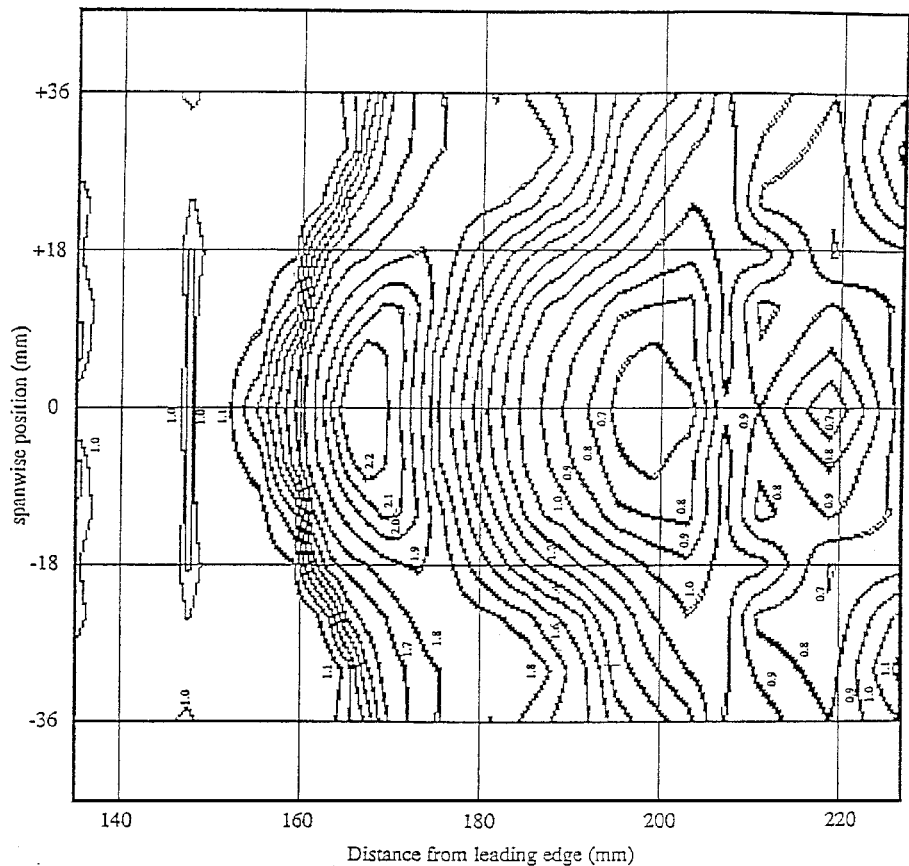


a) $\theta_c = 14$ deg



b) $\theta_c = 20$ deg

Fig. 7 Surface-pressure contours.



c) $\theta_c = 30\text{ deg}$

Fig. 7 Surface-pressure contours (continued).

edge of the plate. This is about twice the thickness of the side-wall boundary layer at the beginning of the interaction region.

The isobar pattern of the interaction is seen to be quite similar in many respects to that of the blunt fin interactions.² However, it is different to that of swept-shock interactions, where the isobars originate from the leading edge of the shock generator and have a maximum at the shock generator surface.¹⁴ This difference is caused by the fact that, in swept interactions, the shock and the separation lines have a common origin at the leading edge of the shock generator, whereas in conical shock interactions the inviscid shock footprint and separation lines are different.

C. Upstream Influence

Upstream influence is the distance from the point where the incident shock would strike the plate in the absence of the boundary layer to the point where the pressure on the plate begins to rise, the so-called interaction start, caused by the presence of the boundary layer.²

It is possible to trace the hyperbolic footprint of the cone shock on the plate.⁷ Then, from the measured pressure data such as from Fig. 6, we can estimate the streamwise upstream influence caused by the interaction reasonably accurately ($\pm 15\%$ in distance). Figure 8 shows examples of the upstream influence line or interaction start for various semicone angles, drawn based on pressure and oil-flow data. The inviscid shock trace for the respective angles is also indicated on the figure. A distinguishing feature is the curved upstream influence line, which is a consequence of the weakening effect of the shock away from the plane of symmetry. As can be expected, the upstream influence increases with the increase in cone angle, albeit slowly. We also notice that the streamwise extent of the upstream influence is approximately the same at all spanwise stations.

Panov⁴ has shown, without rigorous proof but based on experimental data, that the critical pressure ratio can be expressed as a sum of two components: a two-dimensional component, which is a function of Mach number for a given boundary-layer thickness and cone angle, and a three-dimensional component, which depends princi-

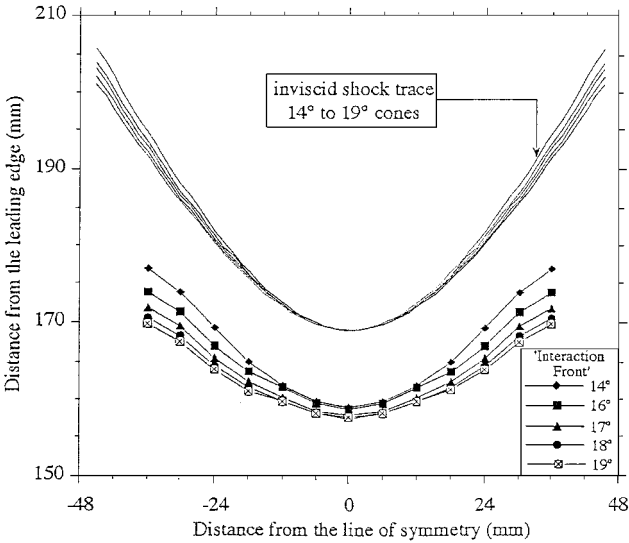


Fig. 8 Inviscid shock trace and upstream influence for various semi-cone angles.

pally on the curvature of the separation line. In the spirit of Panov, one can extend this analogy for the upstream influence also, and we can write

$$L_{u3}/\delta_0 = L_{u2}/\delta_0 - k(\delta_0/R)$$

where L_{u3} and L_{u2} are the three- and two-dimensional streamwise upstream influence distances, R is the radius of the curved upstream influence line in the plane of symmetry, and k is a constant. The second term on the right-hand side of this expression can be considered as a corrective term to take account of the spanwise pressure gradient. Obviously, when $R \rightarrow \infty$, we obtain the two-dimensional result.

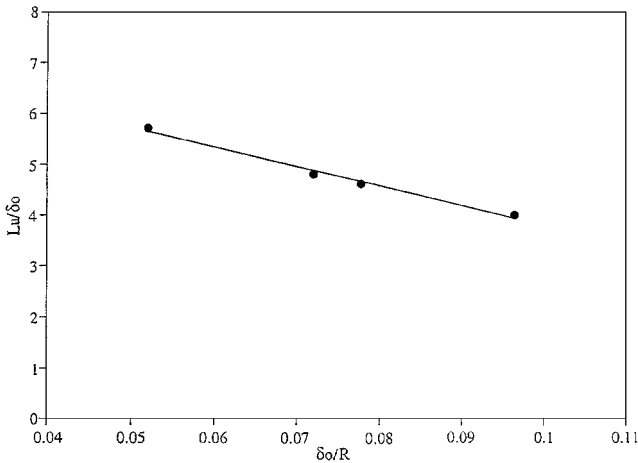


Fig. 9 Streamwise upstream influence vs curvature of the interaction front.

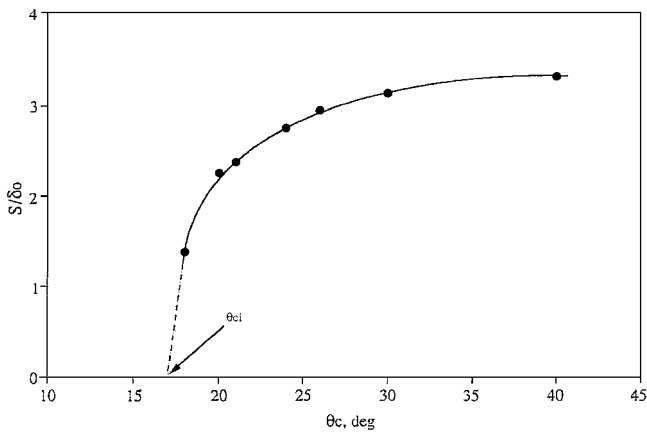


Fig. 10 Separation length vs semicone angle θ_c .

The preceding expression has no theoretical basis but is based on the present experiments and Panov's observations. However, as pointed out by Avduyevskii and Medvedev,¹⁵ for the same initial boundary-layer thickness subjected to interaction the three-dimensional upstream influence is smaller than that of the two-dimensional case because of the lateral pressure gradient (see also discussion by Settles and Dolling²). Figure 9 shows the streamwise upstream influence plotted against the curvature of the interaction front, and the upstream influence decreases with decreasing cone angle, that is, with increasing curvature.

D. Separation

Based on surface oil-flow patterns, separation was identified and measured at the plane of symmetry for various semicone angles. The results are shown in Fig. 10. These measurements are the same as in Fig. 2 for the cone height of 30 mm, except that the separation length s is normalized by the boundary-layer thickness δ_0 at the start of interaction. Extrapolation of data to $s/\delta_0 = 0$ would suggest that incipient separation will occur for a semicone angle of 17 deg approximately. This gives a shock-wave angle of 35.3 deg and a pressure ratio of 1.4. This can be compared with the incipient pressure ratio of 1.6 and 2.2 for the swept shock wave and two-dimensional shock wave and turbulent boundary-layer interactions, respectively.^{2, 12, 16} This is also consistent with the fact that, in general, the incipient separation pressure in a three-dimensional separation is far less than that in a two-dimensional separation. However, in this particular configuration the incipient pressure is also dependent on the height of the cone above the plate, a point made previously by Panov.⁴

IV. Conclusions

This study of an incident conical shock wave and a plane turbulent boundary-layer interaction has provided information on the complex interaction under both attached and separated flow conditions.

The schlieren visualization results showed that the interaction depends strongly on the cone angle and the height of the cone above the plate.

The surface oil-flow studies showed a curved three-dimensional separation, which reduced in size and eventually became negligibly small away from the plane of symmetry. With a large separated region a secondary separation embedded within the primary separation was also observed.

The surface pressure distributions did not reveal either a plateau or a dip when separation occurred. In this respect the results were unlike those of Panov⁴ but similar to those of Kussoy et al.⁵ The surface-pressure contours also showed some similarity to those observed in blunt fin interactions.²

The surface-pressure data revealed strong side-wall influence. The side-wall influence would undoubtedly have corrupted some of the data, but the general agreement of the main features of the interaction with previous similar investigations lends credence to the data presented here.

Both the upstream influence and the incipient separation pressure were found to be less than that for swept and two-dimensional interactions. This is in agreement with previous investigations.

Tests conducted at two different Reynolds numbers, differing by nearly a factor of two, showed no significant differences.

References

- Stollery, J. L., "Glancing Shock-Boundary Layer Interactions," AGARD-VKI Special Course on Three-Dimensional Supersonic and Hypersonic Flows, von Kármán Inst., Brussels, May 1989.
- Settles, G. S., and Dolling, D. S., "Swept Shock Wave/Boundary Layer Interactions," *Tactical Missile Aerodynamics*, edited by M. J. Hemsch, Vol. 141, Progress in Aeronautics and Astronautics, AIAA, Washington, DC, 1992, pp. 505–574.
- Migotsky, E., and Markovin, M. V., "Three-Dimensional Shock Wave Reflections," *Journal of the Aeronautical Sciences*, Vol. 18, No. 7, 1951, pp. 484–489.
- Panov, Yu. A., "Interaction of Incident Three-Dimensional Shock Wave with a Turbulent Boundary Layer," *Fluid Dynamics*, Vol. 3, No. 3, 1968, pp. 108–110.
- Kussoy, M. I., Viegas, J. R., and Horstman, C. C., "Investigation of a Three-Dimensional Shock Wave Separated Turbulent Boundary Layer," *AIAA Journal*, Vol. 18, No. 12, 1980, pp. 1477–1484.
- Brosh, A., Kussoy, M. I., and Hung, C. M., "Experimental and Numerical Investigation of a Shock Wave Impingement on a Cylinder," *AIAA Journal*, Vol. 23, No. 6, 1985, pp. 840–846.
- Teh, S. L., "Interaction of an Incident Conical Shock Wave with a Plane Turbulent Boundary Layer," Ph.D. Dissertation, Mechanical Engineering Dept., Univ. College, Univ. of New South Wales, Canberra, Australia, June 1993.
- Chpoun, A., Passerel, D., Li, H., and Ben-Dor, G., "Reconsideration of Oblique Shock Wave Reflections in Steady Flows; Part 1., Experimental Investigation," *Journal of Fluid Mechanics*, Vol. 301, 1995, pp. 19–35.
- Vuillon, J., Zeitoun, D., and Ben-Dor, G., "Reconsideration of Oblique Shock Wave Reflections; Part 2., Numerical Investigation," *Journal of Fluid Mechanics*, Vol. 301, 1995, pp. 37–50.
- Merzkirch, W., *Flow Visualisation*, Academic, New York, 1987, pp. 134–141.
- Henderson, L. F., "The Reflexion of a Shock Wave at a Rigid Wall in the Presence of a Boundary Layer," *Journal of Fluid Mechanics*, Vol. 30, 1967, pp. 699–722.
- Delery, J. M., "Shock Wave/Turbulent Boundary Layer Interaction and Its Control," *Progress in Aerospace Sciences*, Vol. 22, No. 4, 1985, pp. 209–280.
- Knight, D. D., Garrison, T. J., Settles, G. S., Zheltovodov, A. A., Maksimov, A. I., Shevchenko, A. M., and Vorontsov, S. S., "Asymmetric Crossing Shock Wave/Turbulent Boundary Layer Interaction," *AIAA Journal*, Vol. 33, No. 12, 1995, pp. 2241–2249.
- Kubota, H., and Stollery, J. L., "An Experimental Study of the Interaction Between a Glancing Shock Wave and a Turbulent Boundary Layer," *Journal of Fluid Mechanics*, Vol. 116, 1982, pp. 431–458.
- Avduyevskii, V. S., and Medvedev, K. I., "Effect of Three-Dimensional Flow on Limiting Pressure Differential for Interaction of Boundary Layer with Shock Waves," *Fluid Dynamics*, Vol. 2, No. 2, 1967, pp. 32–34.
- Korkegi, R. H., "A Lower Bound for Three-Dimensional Turbulent Separation in Supersonic Flow," *AIAA Journal*, Vol. 23, No. 3, 1985, pp. 475–476.